Dispersion of Molecular Patterns Written in Turbulent Air

Van De Water, Willem; Dam, Nico; Calzavarini, Enrico

DOI
10.1103/PhysRevLett.129.254501

Publication date
2022

Document Version
Final published version

Published in
Physical review letters

Dispersion of Molecular Patterns Written in Turbulent Air

Willem van de Water*
Laboratory for Aero and Hydrodynamics, Delft University of Technology and J.M. Burgers Centre for Fluid Dynamics, 2628 CD Delft, Netherlands

Nico Dam
Institute for Molecules and Materials, Radboud University, 6500 GL, Nijmegen, Netherlands and Mechanical Engineering Department, Eindhoven University of Technology, P.O. Box 513, 5600 MB Eindhoven, Netherlands

Enrico Calzavarini
Université de Lille, ULR 7512-Unité de Mécanique de Lille Joseph Boussinesq (UML), F-59000 Lille, France

(Received 10 June 2022; revised 11 October 2022; accepted 8 November 2022; published 14 December 2022)

We study the dispersion of tiny molecular clouds in turbulence by writing patterns in turbulent air and following their deformation in time. The writing is done by fusing O_2 and N_2 molecules into NO in the focus of a strong ultraviolet laser beam. By crossing several of these laser beams, patterns that have both small and large scales can be painted. The patterns are visualized a while later by inducing fluorescence of the NO molecules with a second UV laser and registering the image. The width of the lines that make the pattern is approximately 50 μm, a few times the Kolmogorov length η, the smallest length scale in turbulence, while the overall size of the patterns (≈4 mm) is inside the inertial range of the used turbulent jet flow. At small scales molecular clouds disperse under the joint action of molecular diffusion and turbulence. The experiments reveal for the first time this subtle, yet very important interaction. At macroscales (≈200 η) we verify the Batchelor dispersion of objects whose size is inside the inertial range; however, the expected influence of molecular diffusion is smaller than the accuracy of the experiments.

DOI: 10.1103/PhysRevLett.129.254501

Introduction.—Turbulence is the erratic flow of a gas or a fluid which mixes added contaminants extremely efficiently. Turbulent motion is characterized by a range of spatial scales which goes from the largest stirred scale to the smallest one, the Kolmogorov scale η, where the scale-to-scale energy flux ϵ is dissipated by molecular viscosity. The intermediate scales are called the inertial range, characterized by an algebraic scale dependence of turbulence statistics. Turbulent mixing on the smallest scales is crucial for chemical reactions such as combustion [1]. Whether a reaction proceeds efficiently or not depends on how well the reactants are mixed on these scales.

In this Letter we study turbulent mixing on small to inertial-range scales by observing how patterns written in a strongly turbulent air flow diffuse and distort. These patterns—tiny clouds—are created from the molecules of the gas themselves. This provides a unique view on the dynamics of turbulent mixing. The patterns are written by weakly focusing UV laser beams with a wavelength of 193 nm in a turbulent air flow emerging from a jet, and fusing the O_2 and N_2 molecules into the long-lived molecular tracer NO. Tracer molecules are made visible by exciting them with a second laser and observing the UV fluorescence using an intensified camera [2]. Naturally, molecular spectroscopy is a key ingredient of our experimental techniques.

In gases, the ratio of the kinematic viscosity ν (the diffusivity of momentum) over the mass diffusivity D_{mol}, the Schmidt number $\mathrm{Sc} = \nu/D_{\mathrm{mol}}$, is of order 1. Since the smallest structures of the turbulent velocity field are set by viscosity, the smallest spatial structures of tagged molecules are blurred by molecular diffusion in the time they are formed. In our experiment, therefore, the growth of clouds is due to the combined action of turbulence and molecular diffusion. The interaction between these effects is quite subtle, as both may reinforce each other such that their combined effect is more than the sum, or, on the contrary, molecular diffusion may have an adverse effect on turbulent dispersion [3,4].

We believe this is the first time that these effects are being unraveled in an experiment. Contrary to numerical simulations and stochastic models [5–7] we find initial linear in time growth of small clouds. We verify that molecular diffusion aids turbulent dispersion of the cloud size, and attempt measurement of the adverse effect on the dispersion of the cloud's center of mass. Turbulent mixing with $\mathrm{Sc} \approx 1$ is of key relevance for gas phase chemistry, but experiments are rare [8]. Our experiments fit a recent renewed interest

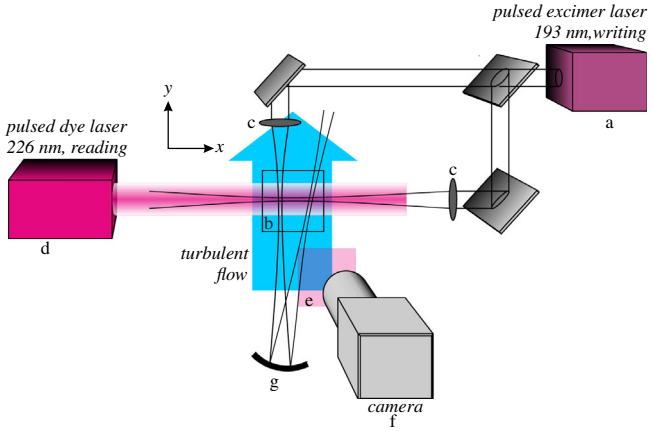

FIG. 1. Experimental setup for writing in air. The beam of an ArF excimer laser (a) at $\lambda = 193$ nm is focused into the 6.4×6.4 mm^2 field of view (b) by lenses (c). A while later the created NO molecules are illuminated by a light pulse from the dye laser (d) at $\lambda = 226$ nm using a broad beam that embraces the written pattern. This wavelength is blocked by an absorption filter (e) which transmits the induced fluorescence. The UV image is registered by a gated, intensified camera (f). By crossing the writing beam several times with a secondary beam (h), using a lens and spherical mirror (g) to focus it, a double cross can be written.

in the interaction between molecular dynamics and turbulence [9,10].

In case of purely diffusive spreading a Gaussian cloud with one-dimensional concentration profile $C(x,t) \propto \exp[-x^2/\sigma^2(t)]$ spreads in time as $\tilde{\sigma}^2(\tilde{t}) = (4/\mathrm{Sc})\tilde{t}$, where the linear size $\sigma(t)$ size of the cloud was made dimensionless with the Kolmogorov length η, $\tilde{\sigma} = \sigma/\eta$, and time t was made dimensionless with the Kolmogorov time τ_η, $\tilde{t} = t/\tau_\eta$. The interaction between turbulence and molecular diffusion results in an extra contribution which is cubic in time, $\tilde{\sigma}^2(\tilde{t}) = (4/\mathrm{Sc})(\tilde{t} + \frac{1}{9}\tilde{t}^3)$. It was first derived by Saffman [3].

At small initial separations, $\delta x(0) \ll \eta$, the distance between two fluid parcels initially grows linearly with time due to the smoothness of the velocity field, $\delta x(t) = (1 + st/\tau_\eta)\delta x(0)$, with s the dimensionless strain rate, $s = \langle(\partial u/\partial y)^2\rangle^{1/2}\tau_\eta = (2/15)^{1/2}$ in homogeneous isotropic turbulence [11,12]. Whether this linear growth survives averaging over turbulence or not depends on the context of the problem: it is absent when the particles are inserted in the flow, and their initial separation vector and the local strain are uncorrelated [12]. It is present in our experiment, where the tagged molecules are an intrinsic part of the flow. The initial linear growth leads to a very simple model for $\sigma(t)$,

$$\tilde{\sigma}^2(t) = \tilde{\sigma}^2(0)(1 + 2s\tilde{t}) + \frac{4}{\mathrm{Sc}}\left(\tilde{t} + \frac{1}{9}\tilde{t}^3\right), \qquad (1)$$

where we added the turbulence-diffusion interaction in an *ad hoc* fashion. It must be compared to the result of a stochastic analysis of Refs. [5,7] which assumes no correlation between the initial particle separation vector and the strain, and where the influence of the turbulence starts with a *quadratic* dependence on time:

$$\tilde{\sigma}^2(\tilde{t}) = \tilde{\sigma}^2(0)\left(1 + \frac{\tilde{t}^2}{3} - \frac{7S_\epsilon}{18\sqrt{15}}\tilde{t}^3\right) + \frac{4}{\mathrm{Sc}}\left(\tilde{t} + \frac{1}{9}\tilde{t}^3\right) \qquad (2)$$

with S_ϵ the dissipation skewness, $S_\epsilon \approx 0.5$ [13,14].

Experiment.—Our experimental setup is sketched in Fig. 1. Two variants of this setup were used. With one single writing laser beam we studied the widening of lines [initial width $\sigma(0) \approx 50$ μm $\approx 3\ \eta$], while with three intersecting laser beams (as shown in Fig. 1), and employing the nonlinearity of the writing process [2] we define two dots whose separation $\Delta \approx 3.4$ mm lies in the inertial range ($\Delta \approx 200\ \eta$), while the dot size is comparable to the beam width δ. By measuring the change of σ and Δ with time, turbulent mixing both on small and large scales is studied in a frame that moves with the flow, the Lagrangian frame.

A strongly turbulent jet flow emerges from a 1 cm diameter nozzle. In the field of view of the camera, 40 nozzle diameters or 0.4 m downstream, the flow is approximately homogeneous and isotropic, with typical mean velocity $U = 40$ m/s, turbulent velocity $u = 10$ m/s (which varies by 2.5% over the field of view), Taylor-scale Reynolds number $R_\lambda = 460$, Kolmogorov scale $\eta \approx 17$ μm, and Kolmogorov time $\tau_\eta \approx 20$ μs.

The wrinkled lines of the deformed patterns are traced using an image processing technique based on active contours which finds their backbone: the ridge of local maximum concentration [16]. Next, the profiles of perpendicular sections of instantaneous lines i are determined by fitting Gaussians to the line intensity $I_i(z,\zeta) = I_i(\zeta)\exp[-z^2/\sigma_i^2(\zeta,t)]$ where z is measured perpendicular to the line center, $\sigma_i(\zeta,t)$ is the line width, ζ is the curvilinear coordinate along the line, and t the time since writing. It is these lines that we view as small-scale clouds; they have a diameter $\sigma_i(\zeta,t)$ comparable to the Kolmogorov scale η. We follow these clouds, and we collect the statistical properties of $\sigma_i(\zeta,t)$ for increasing delay time t.

The nitric oxide tracer molecules which are created in this experiment have a molecular mass that is comparable to that of the indigenous air molecules. With molecular diffusivity $D_{\mathrm{mol}} = 2.42 \times 10^{-5}$ m^2 s^{-1} and kinematic viscosity of air, $\nu = 1.5 \times 10^{-5}$ m^2 s^{-1}, the Schmidt number is $\mathrm{Sc} = \nu/D_{\mathrm{mol}} = 0.62$.

Effective diffusion.—The linear approximation of Eq. (1) defines an effective diffusion coefficient D_{eff}, $\sigma^2(t) = \sigma^2(0) + 4D_{\mathrm{eff}}t$, with

$$D_{\mathrm{eff}} = D_{\mathrm{mol}} + \sigma^2(0)s/2\tau_\eta, \qquad (3)$$

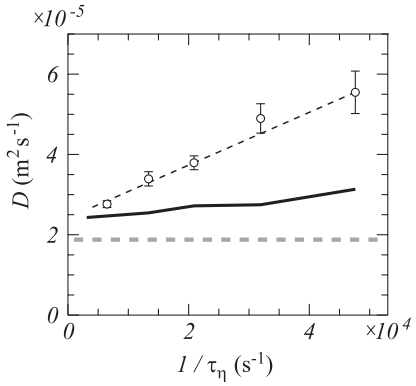

FIG. 2. Effective diffusion coefficient from short-time line broadening. Dots, experiment; $D_{\rm eff} = (\langle\sigma^2(t)\rangle - \langle\sigma^2(0)\rangle)/4t$ measured from the width of lines for a range of turbulent velocities u, with the observation time ranging from $t/\tau_\eta = 0.1$ to $t/\tau_\eta = 0.5$. The error bars are the rms variation of $D_{\rm eff}$ along the written line. Dashed line, Eq. (3). Solid line, $D_{\rm eff}$ using Eq. (2). Gray dashed line, literature value of $D_{\rm mol}$ [17]. The turbulent velocity u determines the Kolmogorov time τ_η, via the turbulent dissipation ϵ, $\tau_\eta = (\nu/\epsilon)^{1/2}$, with ν the kinematic viscosity, and where the relation between u and ϵ was established in a separate experiment.

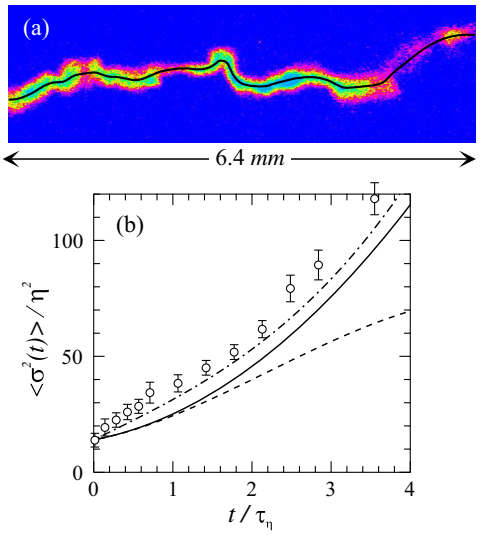

FIG. 3. The widening of lines written in a strongly turbulent flow is due to both molecular diffusion and turbulent dispersion. (a) The line has been registered at time $t = 35$ μs after it was written. It is shown together with a fit $\boldsymbol{x}(\zeta)$ of its backbone; these fits were made using the technique of active contours [16]. (b) Symbols, squared Gaussian width $\langle\sigma^2(t)\rangle$. The error bars are the rms variation of the time-averaged σ over the extent of the line. Full line, prediction of Eq. (2) [7]. Dashed line, Eq. (2) without the interaction term $\frac{1}{9}\tilde{t}^3$. Dash-dotted line, prediction of Eq. (1).

where $D_{\rm mol}$ is the molecular diffusion coefficient. The effective diffusion coefficient depends on the turbulence intensity through the Kolmogorov timescale τ_η; in quiescent flow, $D_{\rm eff} = D_{\rm mol}$.

We measured the dependence of $D_{\rm eff}$ on the turbulence intensity through the widening of lines in an experiment where we varied the flow velocity of the jet, $D_{\rm eff} = (\langle\sigma_i^2(t)\rangle - \langle\sigma_i^2(0)\rangle)/4t$, where t ranges from $t = 0.1\tau_\eta$ at the smallest turbulent velocity u, to $t = 0.5\tau_\eta$ at the largest u. An average is done over $\approx 10^3$ lines i and over the extent of lines.

We compare the experimental result, shown in Fig. 2, to finite differences computed from the simple model [Eq. (3)], and from Eq. (2). At these small times t the influence of the interaction term is negligible. The simple model agrees well with the data, while there is a large difference with the prediction of Eq. (2). This discrepancy owes itself to the absence of a term linear in t in Eq. (2).

For vanishing turbulence, $u \to 0$, $D_{\rm eff}$ tends to $D_{\rm mol} = 2.42 \times 10^{-5}$ m^2 s^{-1}. The molecular diffusion coefficient $D_{\rm mol}$ is larger than the literature value for the diffusion of NO in air, $D_{\rm mol} = 1.99 \times 10^{-5}$ m^2 s^{-1} [17]. This is due to the heat released in the tagging process [2].

Cloud dispersion at long times.—To observe the widening of lines over long times (a few times τ_η) we have written single straight lines i in a strongly turbulent flow ($R_\lambda = 460$) and measured their average squared width $\langle\sigma_i^2(\zeta, t)\rangle$, as a function of the delay time t between writing and reading. Averages $\langle\rangle$ were done over 4×10^3 lines, and over the extent of each individual line.

Figure 3 shows the experimental results, which are compared to Eq. (2) [7], and to the simple model [Eq. (1)]. For short delay times Eq. (2) disagrees with the experiment, consistent with the result in Fig. 2. For longer delay times both models, Eqs. (1) and (2), are in fair agreement with the experiment, an agreement which owes itself to the $\propto \tilde{t}^3$ interaction term. Thus, this experiment demonstrates the constructive interaction between molecular diffusion and turbulent dispersion.

Dispersion of 3D blobs.—The creation of the NO tracer molecules through irradiation by an intense UV laser is a nonlinear process, with the tagged NO molecule concentration depending quadratically on the laser intensity [2]. This offers the opportunity to write three-dimensional blobs in the perpendicular intersection region of two laser beams.

Assuming Gaussian beam profiles with Gaussian widths σ, the concentration profile of a blob with center $\boldsymbol{x} = 0$ is $C(x, y) = C_0[\exp(-x^2/\sigma^2) + \exp(-y^2/\sigma^2)]^\beta$, with the measured NO fluorescence profile proportional to $C(x, y)$, and $\beta = 1$ in the case that the written concentrations may simply be added while $\beta = 2$ for a writing process with quadratic nonlinearity. These two cases are illustrated in Fig. 4(a). For $\beta = 2$, the NO concentration profile has the shape of a cross with a highlighted center which is approximately Gaussian. In the analysis of the fluorescence NO images, the lines and their intersections were found using the technique of active contours [16], after which the function $C(x, y)$ was fitted to the intersection region with

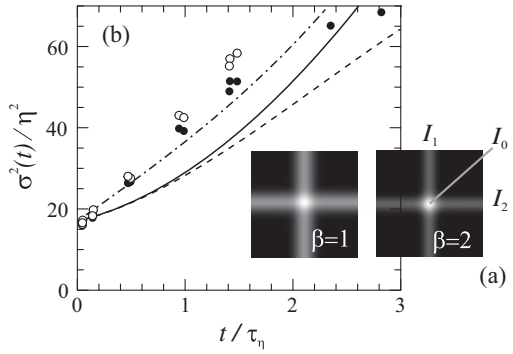

FIG. 4. The widening of dots in a turbulent flow. The dots are small molecular clouds that were created at the intersection of two laser beams, using the nonlinearity of NO formation. (a) Influence of the nonlinearity of the writing process. The intensities of the crossing lines are I_1 and I_2, while I_0 is the intensity of the intersection point. (b) Open circles, $\langle\sigma^2(t)\rangle$; the closed dots show the influence of the deformation of the cross due to turbulence, $\langle\sigma^2(t)\sin^2(\alpha_2-\alpha_1-\pi/2)\rangle$. The statistical uncertainty is smaller than the symbol size. Full line, prediction of Eq. (2) [7]. Dashed line, Eq. (2) without the interaction term $\frac{1}{9}\tilde{t}^3$. Dash-dotted line, prediction of Eq. (1).

the parameters C_0, σ, α_1 and α_2 determined in a least squares procedure. The intensity profile $C(x, y)$ with $\beta = 2$ is not a simple Gaussian. Because of the nonlinearity, the fitted σ overestimates the true width.

Our laser beams are a mere 50 μm wide, and crossing them exactly in space is a challenge. The degree of spatial overlap can be monitored by a measurement of the fluorescence intensity I_0 in the intersection point, compared with $I_{1,2}$ of the crossing lines (see Fig. 4). In the case of perfect overlap and quadratic nonlinearity, the quantity $I_0/(I_1 + I_2) = 2$ (in the case that $I_1 = I_2$). We find a fair degree of overlap with an average ratio $I_0/(I_1 + I_2) = 1.5 \pm 0.4$, where the error is the root-mean-square fluctuation; consequently, we fix $\beta = 2$ in our analysis.

The result for σ^2 as a function of delay time is shown in Fig. 4(b), together with the predictions of Eqs. (2) and (1). The conclusion agrees with that for the spreading of lines: the discrepancy with the model [Eq. (2)] at small times is again evident, while both models highlight the importance of the interaction contribution.

Turbulent dispersion at inertial-range scales.—A surprising consequence of the interaction of molecular diffusion with turbulence is that the dispersion of the center of mass of molecular clouds lags behind the dispersion of fluid parcels [3].

In our experiment we write a double cross, with $\Delta(t)$ the separation of its nodes [see Fig. 5(a)]. Because the lines broaden as time progresses, the $\Delta(t)$ that we measure is not the separation of two material points of the flow, but the distance between the centers of mass of the intersection regions whose size grows to $\approx 10\ \eta$ at the longest delay times.

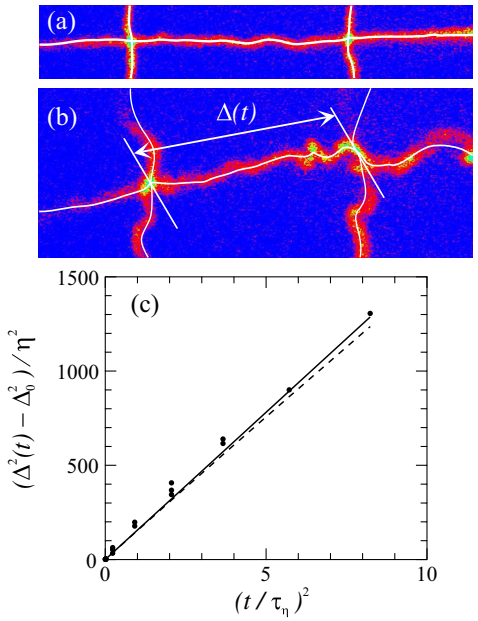

FIG. 5. The dispersion of two dots in turbulence that at $t = 0$ have an inertial-range separation $\Delta_0 = 200\ \eta$. The separation $\Delta(t)$ is defined as the distance between the intersection points of three lines written in a turbulent flow. (a) Image of double cross, $t = 10$ μs after it was written, (b) delay time of $t = 40$ μs. (c) Dots, measured $\langle\Delta^2(t)\rangle - \Delta_0^2$ as function of delay time t. Line, prediction of the Batchelor formula [Eq. (4)]. Dashed line, Batchelor formula including interaction of diffusion and turbulence.

In the absence of diffusion, the distance between two material points $\boldsymbol{x}_1$, $\boldsymbol{x}_2$, which are initially separated by $|\boldsymbol{x}_2 - \boldsymbol{x}_1| = \Delta_0$ in the inertial range, grows in time according to the well-known Batchelor prediction [15]. In dimensionless units,

$$\langle\tilde{\Delta}^2(t)\rangle - \tilde{\Delta}_0^2 = \frac{11}{3} C_2 \tilde{\Delta}_0^{2/3} \tilde{t}^2, \tag{4}$$

where $C_2 \approx 2.1$ [18] is the universal constant of the inertial-range scaling law of the longitudinal second-order Eulerian structure function, $\langle[(\boldsymbol{u}_2 - \boldsymbol{u}_1)\cdot\boldsymbol{\Delta}_0/\Delta_0]^2\rangle = C_2\epsilon^{2/3}\Delta_0^{2/3}$, and the factor $11/3$ owes itself to the isotropy of the velocity field. The Batchelor formula expresses the short-time ballistic motion of two material points whose initial separation is inside the inertial range. When these points are the centers of mass of molecular clouds, diffusion slows down $\langle\tilde{\Delta}^2(t)\rangle$ by $4\tilde{t}^3/3$ Sc [3].

In the quest for the interaction effect, but now at inertial-range length scales, we wrote 4×10^3 double crosses at each delay time t in the turbulent jet flow. From the images we collected the statistics of $\boldsymbol{\Delta}(t) = \boldsymbol{x}_2 - \boldsymbol{x}_1$, with the reference Δ_0 taken as the mean $|\langle\boldsymbol{\Delta}_i(t=0)\rangle_i|$. The results are shown in Fig. 5(b), and compared with Batchelor's prediction [Eq. (4)], including the diffusion term $-4\tilde{t}^3/3$ Sc. Because we measure $\Delta(t)$ in a two-dimensional projection of the

actual separation, the isotropy factor 11/3 in Eq. (4) now becomes 7/3.

The predicted lag of the cloud's centers of mass is a mere 4% at the largest time delay, which is smaller than the accuracy of the experiment. Otherwise, the dot separation agrees well with Batchelor's formula [Eq. (4)]. We emphasize that the computation of Batchelor's prediction does not involve adjustable parameters; the dissipation rate ϵ was measured in a separate experiment. The statistical error of $\langle \Delta^2(t) \rangle - \Delta_0^2$ is smaller than the size of the dots in Fig. 5. What remains are systematic errors due to the pointing stability of the laser beams.

Conclusion.—Molecular tagging in a turbulent gas can be used for velocimetry [19,20], but it fundamentally cannot resolve motion on the smallest scales due to the interaction with diffusion [2]. However, tagging molecules opens up a unique view on small-scale turbulent mixing.

The structures that we write in a strongly turbulent flow probe the initial episode of turbulent mixing. It is characterized by the subtle interplay between molecular diffusion and turbulent strain: without diffusion two very close points would take a long time to separate to the Kolmogorov scale. Once the cloud becomes sizable, turbulent dispersion takes over. It is only in the Lagrangian frame—the context of this experiment—that these interaction effects can be tested.

We gratefully acknowledge financial support by the Dutch Research Council. We are indebted to Mira Pashtrapanska for the results on the two-dot dispersion. We also thank Mehrnoosh Mirzaei for performing experiments.

*Corresponding author.
w.vandewater@tudelft.nl

[1] A. M. Steinberg, P. E. Hamlington, and X. Zhao, Structure and dynamics of highly turbulent premixed combustion, Prog. Energy Combust. Sci. **85**, 100900 (2021).
[2] J. Bominaar, T. Elenbaas, M. Pashtrapanska, N. Dam, J. J. ter Meulen, and W. van de Water, Writing in turbulent air, Phys. Rev. E **77**, 046312 (2008).
[3] P. G. Saffman, On the effect of the molecular diffusivity in turbulent diffusion, J. Fluid Mech. **8**, 273 (1960).
[4] A. Mazzino and M. Vergassola, Interference between turbulent and molecular diffusion, Europhys. Lett. **37**, 535 (1997).
[5] B. L. Sawford and J. C. R. Hunt, Effects of turbulence structure, molecular diffusion and source size on scalar fluctuations in homogeneous turbulence, J. Fluid Mech. **165**, 373 (1986).
[6] D. Buaria, B. L. Sawford, and P. K. Yeung, Characteristics of backward and forward two-particle relative dispersion in turbulence at different Reynolds numbers, Phys. Fluids **27**, 105101 (2015).
[7] D. Buaria, P. K. Yeung, and B. L. Sawford, A Lagrangian study of turbulent mixing: Forward and backward dispersion of molecular trajectories in isotropic turbulence, J. Fluid Mech. **799**, 352 (2016).
[8] K. A. Buch and W. J. A. Dahm, Experimental study of the fine-scale structure of conserved scalar mixing in turbulent shear flows. Part 2. Sc $\approx$ 1, J. Fluid Mech. **364**, 1 (1998).
[9] G. Eyink, D. Bandak, N. Goldenfield, and A. A. Mailybaev, Dissipation-range turbulence and thermal noise, arXiv: 2107.13954v1.
[10] R. M. McMullen, M. C. Krygier, J. R. Torczynski, and M. A. Gallis, Navier-Stokes Equations Do Not Describe the Smallest Scales of Turbulence in Gases, Phys. Rev. Lett. **128**, 114501 (2022).
[11] G. K. Batchelor, The effect of homogeneous turbulence on material lines and surfaces, Proc. R. Soc. A **213**, 349 (1952).
[12] R. Dhariwal and A. D. Bragg, Fluid particles only separate exponentially in the dissipation range after extremely long times, Phys. Rev. Fluids **3**, 034604 (2018).
[13] R. M. Kerr, Higher-order derivative correlations and the alignment of small-scale structures in isotropic numerical turbulence, J. Fluid Mech. **153**, 31 (1985).
[14] Note that Eq. (2.17) in [7] is for the squared separation of molecular pairs, which is *twice* the squared cloud size [15]. On the other hand, the squared Gaussian width σ^2 is *half* the squared cloud size. Also, Eq. (2.17) in [7] is for the particle separation in three dimensions whereas we consider one-dimensional Gaussian cross sections, which leads to a factor 3. In summary, there is a factor 3 between the second term on the right hand side of Eq. (2) and the corresponding term in Eq. (2.17) of [7].
[15] G. K. Batchelor, Diffusion in a field of homogeneous turbulence: II the relative motion of particles, Proc. Cambridge Philos. Soc. **48**, 345 (1952).
[16] W. van de Water and N. Dam, How to find patterns written in turbulent air, Exp. Fluids **54**, 1574 (2013).
[17] W. J. Massman, A review of the molecular diffusivities of H_2O, CO_2, CH_4, CO, O_3, SO_2, NH_3, N_2O, NO, in air, O_2 and N_2 near STP, Atmos. Environ. **32**, 1111 (1998).
[18] K. R. Sreenivasan, On the universality of the Kolmogorov constant, Phys. Fluids **7**, 2778 (1995).
[19] A. Noullez, G. Wallace, W. Lempert, R. B. Miles, and U. Frisch, Transverse velocity increments in turbulent flow using the relief technique, J. Fluid Mech. **339**, 287 (1997).
[20] B. Stier and M. M. Koochesfahani, Molecular tagging velocimetry (MTV) measurements in gas phase flows, Exp. Fluids **26**, 297 (1999).